J MATER SCI 41 (2006) 3761–3766

Microstructure and growth mechanism of stressed complex oxide thin films in strain-modulation

J. L. LI*, Y. RONG LI, J. ZHU, Y. ZHANG
School of Microelectronics Engineering, University of Electronics Science and Technology of China, Chengdu 610054, People Republic of China

F. YANG, W. FEI
School of Material Science and Engineering, Harbin Institute of Technology, Harbin 150001, People Republic China

Published online: 10 April 2006

A series of experiments of strain modulations in heterostructures of $SrTiO_3$/$LaAlO_3$ and $LaAlO_3$/$SrTiO_3$ perovskite thin films fabricated by laser molecular beam epitaxy (L-MBE) were performed to study the effect of the compressive stress and tensile stress on the growth and microstructure of the films. The growth process of the films was *in-situ* monitored by reflective high-energy electron diffraction (RHEED). The morphology of the films was studied by *ex-situ* atomic force microscopy (AFM). We demonstrated that the compressive stress-induced self-organized $SrTiO_3$ films deposited on $LaAlO_3$ (100) single crystal substrates exhibited a periodic well-ordered ripple-shaped structure, forming a unique nanopatterning tool to fabricate 1D/2D arrays of confined nanostructures (i.e., islands and wires). Small angle X-ray scattering technique was employed to investigate the superstructure. Symmetric satellite peaks were observed, which also revealed the well-aligned self-organized structures. In contrast, the similar superstructure was not observed during the growth of the tensile stress-induced $LaAlO_3$ films on $SrTiO_3$ substrates. Based on the experimental data, the compressive stress was estimated as the main reason of the self-organized growth. A growth model about the formation mechanisms of compressive stress-induced nanostructure was put forward and systematical kinetics elucidations about the growth processes were also discussed to illustrate the effects of different stresses on the growth and microstructures of the films.

1. Introduction

Motivated by the novel properties and their increasing technological interest (note for instance, the crucial advances in high-*Tc* superconductors, ferroelectrics and colossal magnetoresistors) based on the confinement effect, more extensive technological and scientific attention was paid to a new emerging oxide-based nanotechnology [1–4]. Through controlled strain engineering, the fabrication by strain-induced self-organizing routes of ordered arrays of spatially-confined inorganic nanostructures constitutes currently one of the frontier subjects in the field of the nanotechnology [2–5]. However, the physical mechanisms and that drive self-organized growth have been studied in details only for semiconductors, but not systematically for complex oxides thin film. Perovskite $SrTiO_3$ thin films have been intensively investigated for their applications to ultrathin gate oxide [6–8] and electrically tunable microwave devices [9, 10]. Recently, with the strain-modulation in the $SrTiO_3$ film, which is not normally ferroelectric at any temperature, the ferroelectric transition temperature (*Tc*) were increased by hundreds of degrees, and the room-temperature ferroelectricity was obtained, which are detrimental to tunability and microwave devices performance [1]. Obviously, strain in the ferroelectric films plays a significant role in influencing their microstructures, as well as the dielectric properties, which are important for electronic applications. The influences of stresses to the films growth and their

*Author to whom all correspondence should be addressed.
0022-2461
DOI: 10.1007/s10853-005-5602-8

microstructures are complex, and a clear understanding of the nature of stresses is of both scientific and technological significance. Some studies about the effect of the temperature on the lattice constants and strain relaxation process during the growth of the film at the growing temperature were made [11–13]. However, systematic studies about different influence of the compressive stress and tensile stress on the films structure and the growth are so far lacking.

In this letter, we fabricated the $SrTiO_3/LaAlO_3$ and $LaAlO_3/SrTiO_3$ heterostructures, respectively, via proper modulation of strains to study the effects of the compressive stress and tensile stress on the films growth and their microstructures. By the compressive stress-induced self-organization of $SrTiO_3$ films, the well-aligned periodic nanostructures were fabricated. A growth dynamic model and systematical illustrations were put forward to express the effects of different stresses on the films for better comprehension of the strain mechanism in the heterostructures.

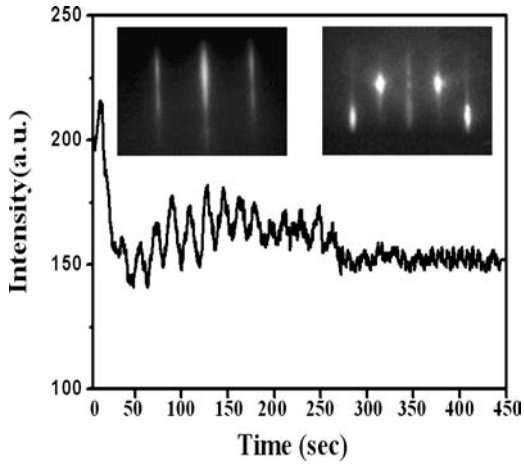

Figure 1 RHEED intensity oscillations and patterns of $SrTiO_3$ thin films grown on $LaAlO_3$ (100) substrate (in the left inset: the initial streaky RHEED patterns in 2D layer-by-layer growth mode, in the right inset: the later spotty plus streaky RHEED patterns in 3D island growth mode, below: the corresponding RHEED intensity oscillations).

2. Experiment

The heteroepitaxial $SrTiO_3$ and $LaAlO_3$ films were fabricated on $LaAlO_3$ (100) and $SrTiO_3$ (100) single crystal substrates, respectively, with laser molecular beam epitaxy (LMBE) using KrF ($\lambda = 248$ nm) excimer laser (LAMBDA PHYSIK, 2 J/cm^2 and 3 Hz). The depositions were made in high vacuum chamber (base vacuum pressure: 1×10^{-5} Pa) at 650°C substrate temperature. The reflective high-energy electron diffraction (RHEED) system was used for *in-situ* monitoring the film growth. The morphology of the films was characterized by atomic force microscopy (AFM, SPA-300 HV, SEIKO). Small angle X-ray scattering (SAXS) technique was carried out to investigate the surface structure of $SrTiO_3$ films grown on $LaAlO_3$ substrate. The θ–2θ scan and ω scan at a small angle were performed in a X'Pert Philips diffractometer using Cu Kα radiation.

$SrTiO_3$ (100) and $LaAlO_3$ (100) single crystal substrates with small miscut angles (0.2°) were selected for this experiment to exclude step-flow like growth behavior to obtain highly atomic smooth surface, which were confirmed by AFM images in our previous work [14]. Before deposition, the substrates were in-situ annealed at the temperature of 800°C to get a carbon-free and high- crystalline surface without other special morphology [3, 14]. Since the room-temperature lattice constant of $SrTiO_3$ and $LaAlO_3$ are 0.3905 nm and 0.379 nm, respectively, one expects the mismatch stress in the $SrTiO_3$ films to be compressive on $LaAlO_3$, while in the $LaAlO_3$ films to be tensile on $SrTiO_3$.

3. Results and discussion

The RHEED patterns and intensity oscillations obtained during the $SrTiO_3$ film growth on $LaAlO_3$ (100) substrate were showed in Fig. 1. In the initial growth stage of the film, the bright streaky RHEED patterns shown in the left inset and the corresponding undamped intensity oscillation of the $SrTiO_3$ film were observed. The RHEED patterns had clear bright 1×1 streaks, indicating that the films had an atomic flatness and single-phase perovskite structure. One period of oscillation corresponded to the growth of one unit cell of $SrTiO_3$, which meant that the film growth proceeded in the 2 dimensions (2D) layer-by-layer fashion. With film thickness increasing, the amplitude of the oscillations decreased, no significant recovery behavior was achieved and the spotty plus streaky RHEED patterns appeared, which was shown in the right inset. This indicated a transition from initial 2D layer-by-layer growth mode to 3 dimensions (3D) growth fashion after a few monolayers [14].

Fig. 2 showed the morphologic evolution of the $SrTiO_3$ films obtained from different growth stage. The $SrTiO_3$ film grown on flat $LaAlO_3$ substrate [Fig. 2a] with 3.9 nm thickness (about 10 unit cells) [Fig. 2b] showed a periodic ripple structure, which was a result of the relief of stress due to the 3.0% lattice mismatch exiting between the film and the substrate. Since the lattice parameter of $SrTiO_3$ is larger than that of $LaAlO_3$, the stress in the epitaxial $SrTiO_3$ film is compressive. With the film thickness increasing, the film releases stress by creating additional surface roughness.

The ripple structure produced a nonuniform distribution of stress at the surface, where a well-ordered nucleation arrangement was obtained, as shown in Fig. 2b. The interripple regions remained stressed and unfavorable to nucleation, while the peaks of ripple were stress-relaxed, resulting in the formation of nucleation center. As the film thickness increased, mismatch dislocation could be formed, leading to strain relaxation. The dislocation position at the surface could act as the nucleation center. Thus, 3D irregular islands were developed from these nucleation centers with the film thickness of 10.33 nm, as shown in

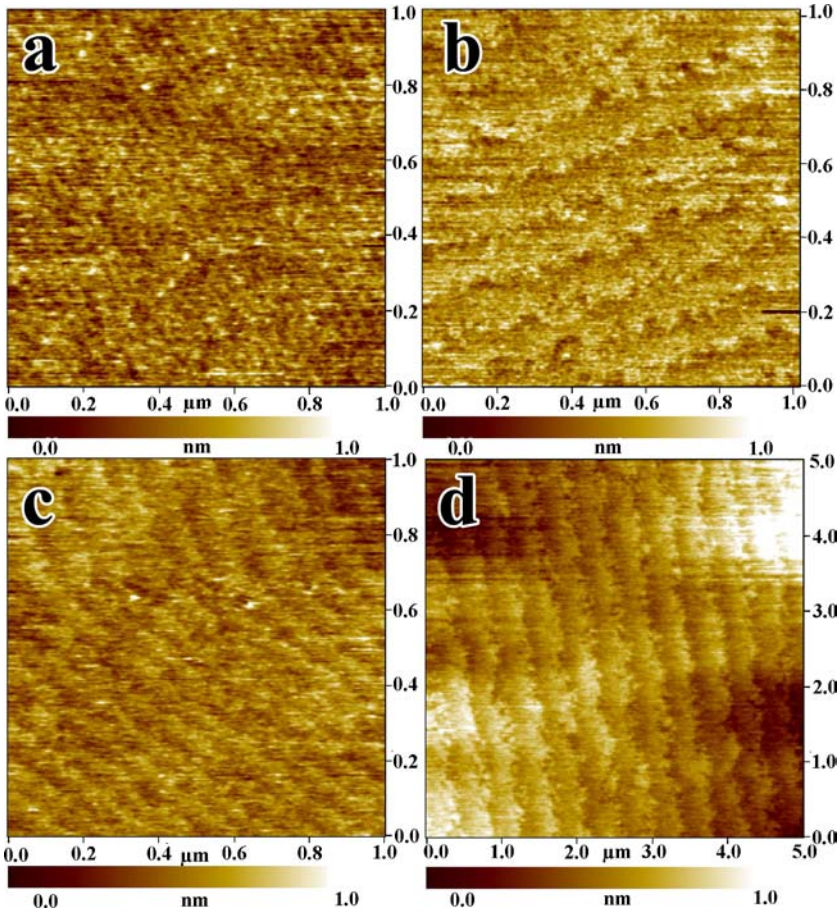

Figure 2 Evolution of the surface morphology AFM images of the self-assembled $SrTiO_3$ films on $LaAlO_3$ with the growth time and the film thickness: (a) (0 nm), (b) (3.9 nm), (c) (10.33 nm), (d) (46.50 nm). The area scanned by AFM was 1 mm × 1 mm^2 in a, b, c and 5 mm × 5 mm^2 in d.

Fig. 2c, which was also in agreement with the RHEED patterns and intensity oscillations obtained at the corresponding stage during the growth, suggesting that the growth proceeded in 3D island growth mode. It was interesting that a well-aligned ripple structure appeared again during the further growth of the film. The in-plane lattice of $SrTiO_3$ had been compressed due to compressive stress. As the 3D growth of the film, the strain had been partially relaxed. When the islands were aligned in more regular continuous form and became nanopattern with a uniform size, the ripple structure occurred again under relatively less compressive stress. Therefore, the distance between the ripples become larger, and streak of ripple was also bigger. Then, the periodic well-ordered ripple-shaped nanostructures were formed as shown in Fig. 2d.

Based on these results, the effects of the compressive stress between the $SrTiO_3$ film and the $LaAlO_3$ substrate should be responsible for the well-aligned self-organized growth of the $SrTiO_3$ films.

In order to investigate the effects of tensile stress on films growth, the $LaAlO_3$ thin films were fabricated on $SrTiO_3$ (100) substrates under the same deposition conditions with the same deposition technique, which were mentioned above in this letter. The $LaAlO_3$ film was drew by tensile stress resulting from the lattice mismatch between $LaAlO_3$ film and $SrTiO_3$ substrate. During the growth process, the RHEED and AFM were also employed. The clear bright streaky RHEED patterns of the $LaAlO_3$ films and undamped intensity oscillations were obtained during the overall deposition, as shown in Fig. 3a, suggesting that the films had an atomic smooth surface. This demonstrated that the film grew in layer-by-layer mode. Fig. 3b also showed the AFM image of $LaAlO_3$ films, which had an atomic flatness with 0.2137 nm RMS. However, ripple structure didn't appear. It was suggested that tensile stress could not result in the formation of a ripple-shaped nanostructure. Tensile stress can enlarge the in-plane lattice of $LaAlO_3$. Consequently, the area of growth surface became larger. The energy of tensile stress can be released by the enhanced surface energy. Thus, the ripple structure did not appear.

In order to further investigate the self-organized structure in the obtained film, SAXS technology was carried out to characterize the nanostructure of $SrTiO_3/LaAlO_3$. θ–2θ scan curve of self-patterned $SrTiO_3$ film on $LaAlO_3$ (100) substrate was shown in Fig. 4a. According to the fluctuation in the curve, the thickness of $SrTiO_3$ film can easily be calculated to be 46.5 nm. Unlike the usual single layer film, there was a peak at the position ($2\theta = 0.8^\circ$).

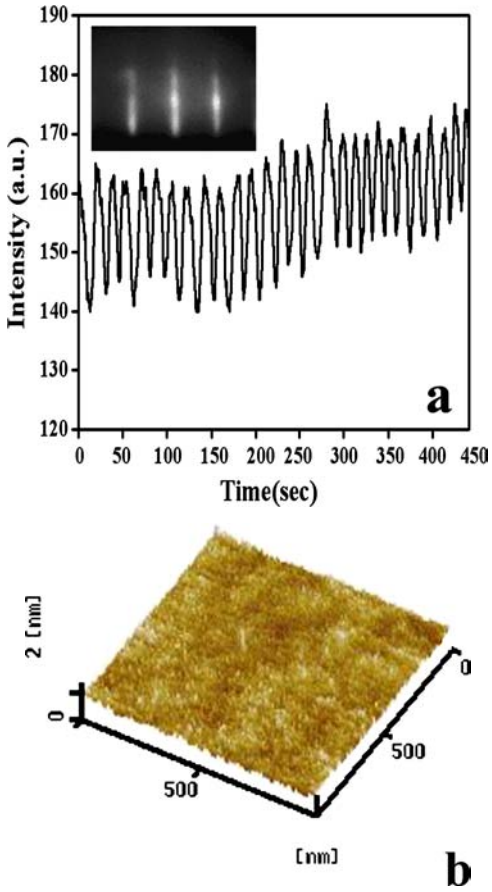

Figure 3 (a) RHEED patterns, intensity oscillations, and (b) AFM images of $LaAlO_3$ thin films on $SrTiO_3$ (100) substrates.

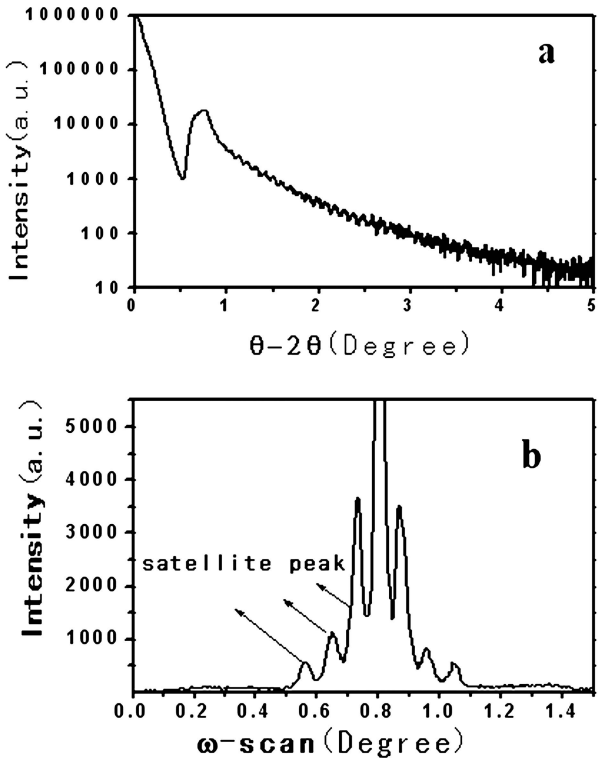

Figure 4 Small angle X-ray scattering of self-patterned $SrTiO_3$ film on $LaAlO_3$ (100): θ–2θ scan curve (a), ω scan curve (b).

It could be concluded that the appearance of the peak at small angle indicated the in-plane self-patterned structure.

The ω scan curve of the self-patterned $SrTiO_3/LaAlO_3$ (100) was shown in Fig. 4b. Symmetric satellite peaks can be clearly observed around the main peak, which demonstrated that the self-organized film had a special periodic structure, since the satellite peaks observed in the rocking scan curve closely demonstrate the well-ordered periodic structure along the out-plane direction. The SAXS results were quite in agreement with our above AFM observations. When the same SAXS method was also employed to characterize the $LaAlO_3/SrTiO_3$ (100) substrate, however, similar phenomena were not observed. SAXS experiments also confirmed that the compressive stress was the main reason to form the well-ordered ripple nanostructure of $SrTiO_3/LaAlO_3$.

Based on the above-mentioned experimental data, the systematical kinetics process of the self-organization caused by compressive stress was suggested. A model about the formation mechanisms of this nanostructure originating from the strain could be put forward.

In the case of $SrTiO_3/LaAlO_3$, $SrTiO_3$ film grow coherently epitaxially on the $LaAlO_3$ substrate in 2D layer-by-layer mode, since the $SrTiO_3$ film was very thin with only a few monolayers, as shown in Fig. 5a [4]. This process was confirmed by the RHEED patterns and intensity oscillations shown in Fig. 1. The compressive stress at this stage was not readily relaxed due to the extremely small film thickness. The film was constrained due to the small difference of lattice parameter between $LaAlO_3$ and $SrTiO_3$. With further growth, the compressive stress could be relaxed by the formation of misfit dislocations in the film, as shown in Fig. 5b. After the formation of misfit dislocation the distributions of stress at the interface was nonuniform. The areas where misfit dislocation located underneath were stressed, where those regions between neighboring misfit dislocations were unconstrained or less constrained. Adatoms on the film surface will form the stress regions to the unstressed regions through a surface diffusion process. With further growth, the compressive stress assembled, while the strain energy decreased with the increasing of the surface energy to achieve the equilibrium state of energy. As a result, a self-nanoassembled rippled structure was formed, as shown in Fig. 5c, which was in agreement with the RHEED oscillations and the observed surface morphology changes, which were shown in Figs. 1 and 2d. The formation of the rippled structure could decrease the strain energy in the film and the system could achieve the minimum of free energy to get the stable energy state. As a result, well-ordered self-organized $SrTiO_3$ film grown on $LaAlO_3$ substrate was fabricated. In the heterostructures of $LaAlO_3/SrTiO_3$, however, during the initial deposition the $LaAlO_3$ film grew coherently epitaxially on the $SrTiO_3$ substrate with 2D layer-by-layer fashion with the thickness thinned as only a few monolayers, which was shown in Fig. 6a. With the $LaAlO_3$ film growth proceeding the film was drew in-plane by tensile stress and there were no strained or unstrained

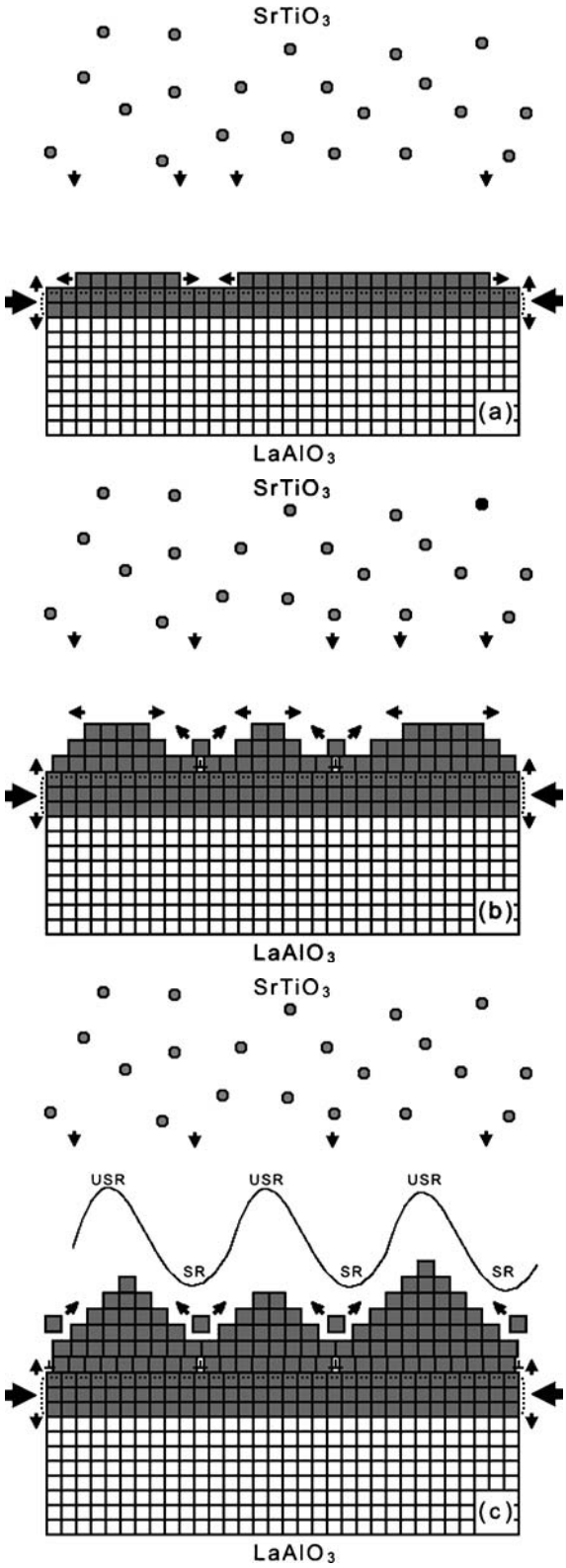

Figure 5 Schematics showing the growth mechanisms of $SrTiO_3$ thin films on the $LaAlO_3$ (100) substrate. (a) $SrTiO_3$ grew in 2D growth mode when the thickness thinned with only a few monolayers; (b) and misfit dislocations formed when the film growth reaches a critical thickness; (c) Formation of ripple-shaped surface structure due to the assembled compressive stress with the stressed regions (SR) to unstressed regions (USR).

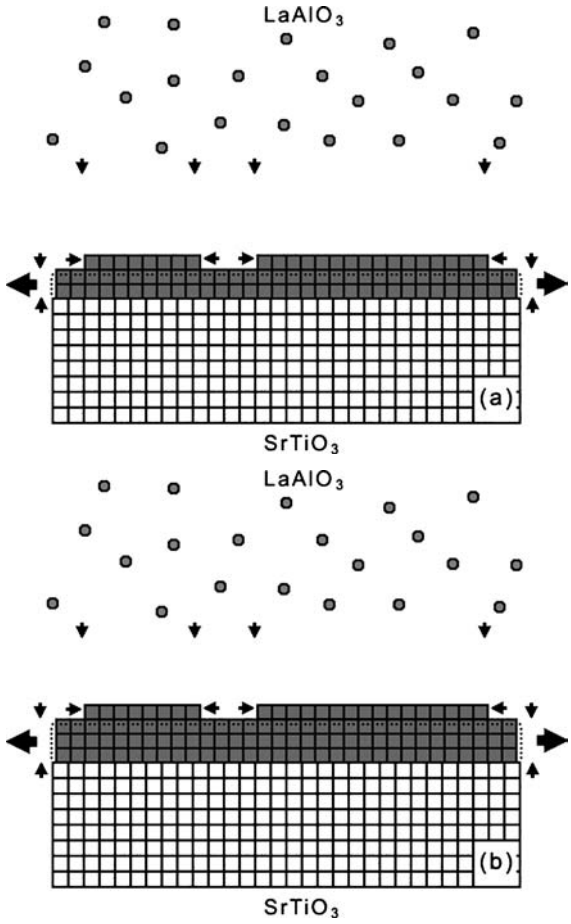

Figure 6 Schematics showing the growth mechanisms of $LaAlO_3$ thin films on the $SrTiO_3$ (100) substrate. (a) 2D growth fashion of $LaAlO_3$ films at the initial stage; (b) The tensile stress relaxed gradually with the increasing of the film thickness and could not take effect on the change of surface structure of the $LaAlO_3$ films.

regions on the surface of the $LaAlO_3$ films, which was different from the compressed $SrTiO_3$ films. The tensile stress, which relaxed gradually with the increasing the film thickness, could not take effect on the change of surface structure of the $LaAlO_3$ films. Thus, an atomically flat surface of $LaAlO_3$ film could be obtained, as shown in Fig. 6b, which are different from that of $SrTiO_3$ films under the otherwise same deposition conditions.

4. Conclusions

In conclusion, through controlled strain engineering, compressive stressed-induced self-organized $SrTiO_3$ films is fabricated on $LaAlO_3$, providing a nanopatterning tool to fabricate 1D/2D arrays of confined nanostructures (i.e., islands and wires). Many methods were employed to characterize the microstructures and growth processes of the films. In terms of strain-modulation, we illustrate the effects of different stresses on the films growth and their microstructures.

References

1. J. H. HAENI, P. IRVIN, W. CHANG, R. UECKER, P. REICHE, Y. L. LI, S. CHOUDHURY, W. TIAN, M. E. HAWLEY, B. CRAIGO, A. K. TAGANTSEV, X. Q. PAN, S. K. STREIFFER, L. Q. CHEN, S. W. KIRCHOEFER, J. LEVY and D. G. SCHLOM, *Nature.* **430** (2004) 758.
2. H. ZHENG, J. WANG, S. E. LOFLAND, Z. MA, L. M. ARDABILI, T. ZHAO, L. S. RIBA, S. R. SHINDE, S. B. OGALE, F. BAI, D. VIEHLAND, Y. JIA, D. G. SCHLOM, M. WUTTIG, A. ROYBURD and R. RAMESH, *Science.* **303** (2004) 661.
3. E. VASCO, R. DITTMANN, S. KARTHAUSER and R. WASER, *Appl. Phys. Lett.* **82** (2003) 2497.
4. J. C. JIANG and X. Q. PAN, *J. Appl. Phys.* **89** (2001) 6365.
5. G. HERRANZ, B. MARTINEZ and J. FONTCUBERTA, *Appl. Phys. Lett.* **82** (2003) 85.
6. Z. YU, J. RAMDANI, J. A. CURLESS, J. M. FINDER, C. D. OVERGAARD, R. DROOPAD, K. W. EISENBEISER, J. A. HALLMARK and W. J. OOMS, *J. Vac. Sci. Technol. B* **18** (2000) 1653.
7. R. A. MCKEE, F. J. WALKER and M. F. CHISHOLM, *Phys. Rev. Lett.* **81** (1998) 3014.
8. P. W. PEACOCK and J. ROBERTSON, *Appl. Phys. Lett.* **83** (2003) 5497.
9. R. OTT, P. LAHL and R. WÖRDENWEBER, *ibid.* **84** (2004) 4147.
10. W. RUIPING and I. MITSURU, *ibid.* **80** (2002) 2964.
11. L. S. J. PENG, X. X. XI and B. H. MOECKLY, *ibid.* **83** (2003) 4592.
12. H. O. SANG and G. P. CHAN, *J. Appl. Phys.* **95** (2004) 4691.
13. J. L. LI, Y. R. LI, Y. ZHANG, X. W. DENG, F. YANG and W. D. FEI, *J. Crys. Grow.* **274** (2005) 612.
14. Y. RONG LI, J. L. LI, Y. ZHANG, X. H. WEI, X. W. DENG and X. Z. LIU, *J. Appl. Phys.* **96** (2004) 1640.

Received 9 March
and accepted 22 July 2005